Ionic liquid-functionalized carbon nanoparticles-modified cathode for efficiency enhancement in polymer solar cells

Xiaohong Chen,[1] Jiaxiang Yang,[1] Jiong Lu,[1] Kiran Kumar Manga,[1] Kian Ping Loh,[1,a] and Furong Zhu[2,a]

[1]*Department of Chemistry, National University of Singapore, 3 Science Drive 3,*
Singapore 117543, Singapore
[2]*Department of Physics and Centre for Advanced Luminescence Materials, Hong Kong Baptist University,*
Kowloon Tong, Hong Kong, Singapore

The power conversion efficiency (PCE) of regioregular poly(3-hexylthiophene) (P3HT) and {6,6}-phenyl C_{61}-butyric acid methylester (PCBM)-based polymer solar cells was increased using an ionic liquid-functionalized carbon nanoparticles (ILCNs) thin film-modified cathode. The PCE of P3HT:PCBM based-polymer solar cells with a conventional aluminum (Al)-only cathode was increased by 20%–30% when the identical devices were made with an ILCNs-modified Al cathode, but its PCE was 10% lower than that of devices with LiF/Al cathode, measured under AM1.5G illumination of 100 mW/cm^2. The ILCN interlayer approach, however, offers practical advantages to LiF in terms of its solution-processability, which is compatible with low cost, large area, and flexible solar cell fabrication. © 2009 American Institute of Physics. [doi:10.1063/1.3237161]

Polymer solar cells are attractive alternatives to silicon-based solar cells due to its scalability toward low cost, large area, and eventually roll-to-roll printing technologies. The cell parameters such as short-circuit current density (J_{sc}), open-circuit voltage (V_{oc}), and fill factor (FF) are affected by a myriad of factors such as the morphology, thickness of the active layer, and work function of electrodes.[1,2] To enhance the performance of polymer solar cells, cathode modifiers such as LiF and Au/LiF (Ref. 3) were thermally deposited on top of active layers before depositing Al cathode. These successive vacuum deposition steps greatly increase the cost and complexity of fabrication. To realize low cost and vacuum-free printing techniques for polymer solar cells, solution processable materials such as TiO_x (Ref. 4) and poly(ethylene oxide)[1] have been developed to modify the cathode for improving the power conversion efficiency (PCE).

Ionic liquids (ILs) have been applied for dye-sensitized solar cells (DSCs) (Ref. 5) due to their unique properties such as negligible vapor pressure, high ionic conductivity, and low toxicity. A quasi-solid-state DSC with an ionic gel electrolyte containing ILs and carbon nanotubes was developed to circumvent the step of hermetic sealing.[5] Conjugated polyelectrolytes have been applied for light-emitting devices.[6,7] Hence, such quasi-solid-state ionic gel electrolyte is expected to be potentially useful in polymer-based solar cells.

We developed an ionic liquid-functionalized carbon nanoparticles (ILCNs) hybrid film, which was synthesized by the electrochemical exfoliation of graphite electrode in 1-butyl-3-methylimidazolium tetrafluoroborate ([C4mim]$^+$[BF4]$^-$) and water mixture (40:60). This modified method produced ILCNs, which is different from previous reports of ionic liquid-functionalized graphene sheets.[8] The shape and size of the exfoliated products can be controlled by tuning the water to IL composition in the electrolyte. The detail chemical and physical experiments and properties will

be reported elsewhere.[9] Such ILCNs consist of ionic liquid molecules and graphitelike carbon nanoparticles held together by hydrogen bonding, van der Waals forces, π-π stacking interactions or/and covalent interactions in a gel-like matrix.[8,10]

The transmission electron microscopy (TEM) images in Fig. 1(a) show that ILCNs are carbon nanoparticles with average sizes below 4 nm. The x-ray photoelectron spectroscopy (XPS) spectrum of the ILCNs is shown in Fig. 1(b), a well-defined peak at 400.9 eV due to the presence of nitrogen (N 1s) can be seen. This peak can be deconvoluted into two components at 400.24 and 401.38 eV, which can be attributed to two different nitrogen bonding environments in
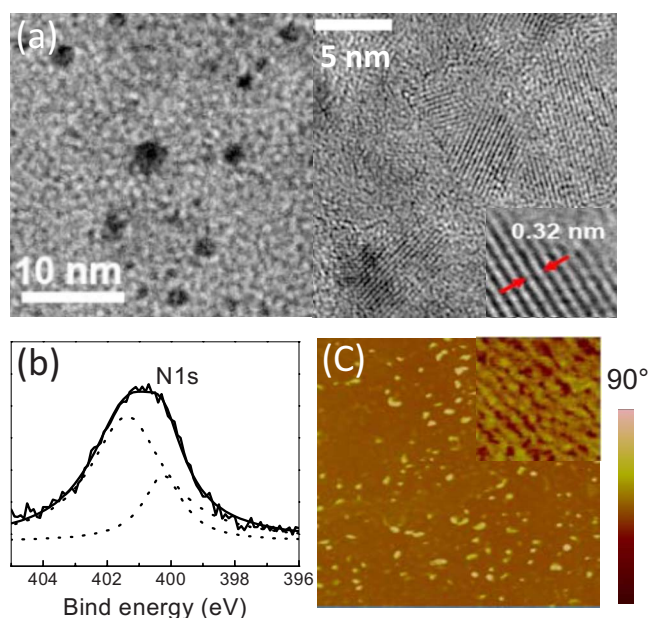

FIG. 1. (Color online) (a) TEM micrographs of ILCNs under different magnifications, (b) XPS N 1s region, (c) AFM phase image of ILCNs on top of the P3HT:PCBM film. The inset in (a) is the High Resolution Transmission Electron Microscopy image, which shows a lattice constant of 0.32 nm for the graphitelike carbon nanoparticles. The inset in (c) is the AFM phase image of pure P3HT:PCBM film.

[a]Authors to whom correspondence should be addressed: Electronic addresses: chmlohkp@nus.edu.sg and frzhu@hkbu.edu.hk.
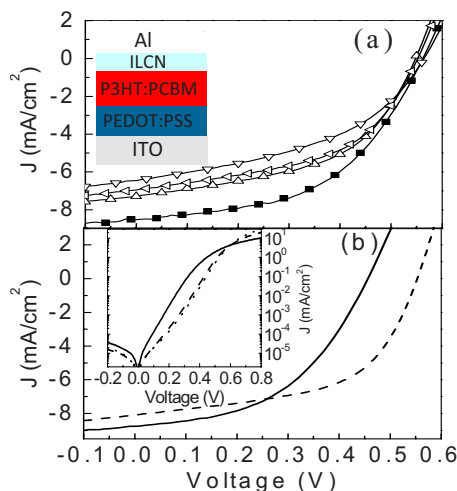
FIG. 2. (Color online) The *J-V* characteristics of different types of the representative device. (a) Device A ($\triangledown$), B ($\triangleleft$), C ($\triangle$), and D ($\blacksquare$) with fast-grown film; (b) device E (solid) and F (dash) with slow-growth film. The inset of (a) is the device structure with ILCN modification. The inset of (b) is the *J-V* curves of devices E (solid), F (dash), and G (dot) in the dark.

TABLE I. Different types of polymer solar cells used in this study.

Device	Cathode	Fabrication condition
A	Al	Fast-grown P3HT:PCBM films. ILCN drop-casted
B	ILCN/Al	onto films to stand for 20 s (B) and 40 s (C) before
C	ILCN/Al	blow drying. The films were annealed at 120 °C
D	LiF/Al	for 5 min again.
E	Al	Slow-grown P3HT:PCBM films. ILCN drop-casted
F	ILCN/Al	onto the films to stand for 40 s before spin coating
G	LiF/Al	on top of blend films in device F.

the imidazolium ion-decorated carbon nanoparticles.[8] The atomic force microscopy (AFM) phase image of ILCNs film is shown in Fig. 1(c). The ILCNs film was fabricated by drop-casting ILCNs solution on top of the blended film of the regioregular poly (3-hexylthiophene) (P3HT) and {6,6}-phenyl C61-butyric acid methylester (PCBM). It is obvious that the phase image of ILCNs-modified P3HT:PCBM films is different from that of pure P3HT:PCBM film [the inset of Fig. 1(c)].

Conjugated carbon materials such as graphene[11] and carbon nanotubes[10] demonstrate superior mechanical properties and electrical conductivities. The sp^2-bonded aromatic structure provides low tunneling barrier height at the interfacial contacts.[12] The ions of ILCNs are expected to form electric double layers with large polarization fields at the interface between the active layer and ILCN, as well as between ILCN and Al cathode.[7] The presence of interfacial electric field helps to reduce the electron injection/extraction barrier. We found that the PCE of polymer P3HT:PCBM-based solar cells using ILCNs-modified cathode can be improved up to 30% compared to that using Al-only cathode measured at AM1.5G illumination of 100 mW/cm^2.

The polymer solar cell structure is shown in the inset of Fig. 2(a). The poly(3,4-ethylenedioxythiophene) poly(styrenesulfonate) (PEDOT:PSS) and P3HT:PCBM thickness were 40 and 200 nm, respectively, and the active area of device was 0.11 cm^2. The PEDOT:PSS (Baytron VPAI4083) was spin coated on top of the Indium Tin Oxide (ITO) substrates (10 Ω sq^{-1}) and then annealed at 140 °C for 15 min under ambient atmospheric condition. P3HT (Sigma Aldrich) and PCBM (American Dye Source) were dissolved in 1,2-dichlorobenzene with 1:0.8 wt. ratio. ILCNs were dissolved in ethanol. P3HT:PCBM films were spin coated on top of PEDOT:PSS film in the glove box (<2 ppm, O$_2$, and H$_2$O). The 0.7 nm thick LiF or/and 100 nm Al metallic layers were thermally deposited with a background pressure of 5 $\times 10^{-7}$ Torr. Current-voltage characteristics were measured in nitrogen under AM1.5G illumination of 100 mW/cm^2 (SAN-EI Electric Xe-Lamp controller). The impedance spectroscopy (IS) data were recorded using an impedance analyzer (Autolab PGSTAT100) in the frequency range of 0.1

Hz–1 MHz at the oscillating voltage of 10 mV.

In order to carry out a systematic study of the effect of the ILCN interlayer on the performance of P3HT:PCBM polymer solar cells, a set of solar cells with four different device architectures was fabricated, as summarized in Table I. For devices A, B, C, and D, the P3HT:PCBM film was spin coated at 800 rpm for 80 s and annealed at 120 °C for 10 min for the fast-growth films. However, the performance of polymer solar cells can be improved by controlling the film morphology with the slow growth method.[2,13] In addition, the V_{oc} and the PCE of polymer solar cells based on pure Al cathode is more sensitive to the Al deposition condition compared to polymer solar cells using modified cathode such as LiF/Al.[14] Therefore, devices E, F, and G were also fabricated with the slow-growth method (Table I). The P3HT:PCBM film was spin coated at 800 rpm for 60 s, and then kept in a petri dish for slow growth. After 12 h, ILCN film was spin coated on top of P3HT:PCBM film and annealed at 120 °C for 10 min.

Figure 2 shows the current density-voltage (*J-V*) curves corresponding to the representative devices. The V_{oc} of device E is only 0.46 V, which is lower than that of device A with V_{oc}=0.56 V. One possible reason is that the samples were heated during the evaporation of Al; this can result in changes to the morphology of the films or to the interface of P3HT:PCBM/Al.[14] However, the V_{oc} of devices based on ILCN or/and LiF-modified electrodes is almost the same even with different Al deposition conditions. The PCE (2.47%) of device F is 29% higher than that (1.91%) of device E. The J_{sc} or/and FF of devices fabricated using the slow-growth method [Fig. 2(b)] are usually higher than the same type of devices made with fast-growth method [Fig. 2(a)]. Our results show that the PCE of polymer solar cells made from the slow-growth method can be greatly improved compared to the same type of devices made from fast-growth method. Figure 3 presents the statistical graphs of characteristics of four types of device with fast growth. From these preliminary data, the PCE of devices based on ILCN layer exhibit improvement in the range of 20%–30% over devices using pure Al electrode, independent of the different film fabrication procedure and Al deposition condition.

The *J-V* curves of the devices in the dark made from the slow-growth method were shown in the inset of Fig. 2(b). The *J-V* curves of devices using Al cathodes exhibited higher reverse and leakage current than identical solar cells made with LiF or ILCN-modified cathode. This reveals that the ILCN and LiF act as protective layers to prevent the diffusion of Al into the active layer.[1] In addition, the short circuit current density measured for the devices made with ILCN or LiF/Al is higher than that of devices with pure Al as a cathode at high forward bias, which indicates the decrease in
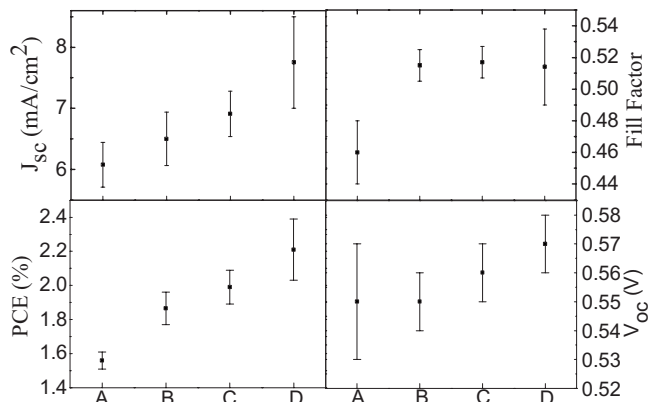
FIG. 3. Device parameters and scatter plot derived from four types of devices with fast-grown film. The cathode composition is Al (device A), ILCN/Al with drop-casted film, which are allowed to stand for 20 s (device B) and 40 s (device C), respectively, and LiF/Al (device D).

interface barrier after cathode modification due to the formation of electric dipole layer.[1,7]

Impedance spectroscopy was also applied to derive insights into the interfacial properties and the charge carrier dynamics of our devices.[15–17] The different contact potential for electrodes modified by different methods is expected to affect carrier collection and carrier accumulation, resulting in differences in the device capacitance. The impedance spectra of three sets of devices in the dark are shown in Fig. 4. The complex impedance plot [Figs. 4(a) and 4(c)] exhibits an arc in the fourth quadrant at the low frequency range at moderate bias voltage (0.5 V), which suggests that negative capacitance exists in device E.[16,17] However, the $-\text{Im}(Z)$ values are always positive at any voltages and frequencies in devices F and G [Figs. 4(b) and 4(d)]. Using the equivalent circuit model in the inset of Fig. 4(c) to fit the Cole–Cole plot, we found that this model is suitable for devices F and G [Figs. 4(b) and 4(d)]. For device E, the fit is good at high voltage of 0.9 V. However the fit is poor at low frequency for moderate voltage of 0.5 V because of its negative capacitance behav-

ior. In the fitting model, R is due to contact resistance at the electrode. The R1C1 semicircle at high frequencies is related to the bulk resistance and the R2C2 semicircle at low frequencies results from the depletion region between the active layer and cathode.[15] The negative capacitive behavior is consistent with reports by Garcia-Belmonte, which attributed it to the Schottky behavior at P3HT:PCBM/Al.[15] In the case of the P3HT:PCBM/Al contact, electron collection might be blocked to some extent due to high barrier height under moderate forward bias, which can result in the negative capacitive behavior when the minority carriers (electrons) are far lower than the dopant density. However, the electron collection barrier of device B and C is low due to the modification by ILCN and LiF, this is consistent with the absence of the negative capacitive phenomenon at the range of voltages and frequencies studied.

In summary, we have demonstrated that the PCE of P3HT:PCBM-based polymer solar cells can be readily improved by 20%–30% by incorporating an ILCN interlayer between polymer blend and Al contact. The ILCN layer can be prepared by drop-casting or spin-coating using an ionic-liquid-functionalized carbon nanoparticles gel. The photocurrent response and IS results measured for polymer solar cells based on modified cathode interfaces, such as ILCN/Al and LiF/AL, indicate that ILCN interlayer plays a similar role as LiF in lowering the electron collection barrier at polymer/cathode interface. The solution-processed ILCN is potentially superior to LiF as a cathode modifier due to its processing compatibility with the fabrication of low cost, large area, and flexible polymer solar cells.
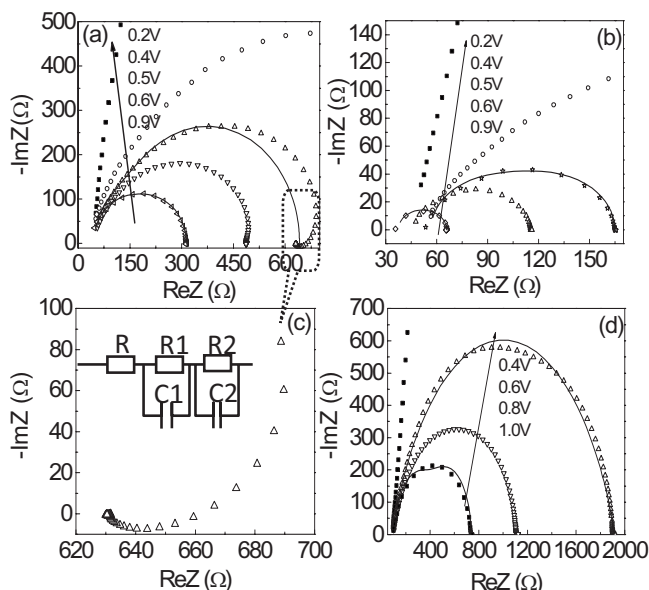
FIG. 4. Bias dependence of Cole–Cole plots of (a) device E, (b) device F, and (d) device G. (c) Zoom in of the Cole–Cole plot. The solid lines are fitting lines from the equivalent circuits in the inset of (c).

[1]F. Zhang, M. Ceder, and O. Inganäs, Adv. Mater. (Weinheim, Ger.) **19**, 1835 (2007).
[2]G. Li, V. Shrotriya, J. Huang, Y. Yao, T. Moriarty, K. Emery, and Y. Yang, Nature Mater. **4**, 864 (2005).
[3]X. Chen, C. Zhao, L. Rothberg, and M. K. Ng, Appl. Phys. Lett. **93**, 123302 (2008).
[4]J. Y. Kim, K. Lee, N. E. Coates, D. Moses, T. Q. Nguyen, M. Dante, and A. J. Heeger, Science **317**, 222 (2007).
[5]H. Usui, H. Matsui, N. Tanabe, and S. Yanagida, J. Photochem. Photobiol., A **164**, 97 (2004).
[6]A. Garcia, R. Yang, Y. Jin, B. Walker, and T. Q. Nguyen, Appl. Phys. Lett. **91**, 153502 (2007).
[7]C. V. Hoven, J. Peet, A. Mikhailovsky, and T. Q. Nguyen, Appl. Phys. Lett. **94**, 033301 (2009).
[8]N. Liu, F. Luo, H. Wu, Y. Liu, C. Zhang, and J. Chen, Adv. Funct. Mater. **18**, 1518 (2008).
[9]J. Lu, J. Yang, J. Wang, A. Lim, S. Wang, and K. P. Loh, ACS Nano **3**, 2367 (2009).
[10]T. Fukushima and T. Aida, Chem.- Eur. J. **13**, 5048 (2007).
[11]A. K. Geim and K. S. Novoselov, Nature Mater. **6**, 183 (2007).
[12]C. Ganzorig, K. J. Kwak, K. Yagi, and M. Fujihira, Appl. Phys. Lett. **79**, 272 (2001).
[13]G. Li, Y. Yao, H. Yang, V. Shrotriya, G. Yang, and Y. Yang, Adv. Funct. Mater. **17**, 1636 (2007).
[14]C. Zhang, S. W. Tong, C. Zhu, C. Jiang, E. T. Kang, and D. S. H. Chan, Appl. Phys. Lett. **94**, 103305 (2009).
[15]G. Garcia-Belmonte, A. Munar, E. M. Barea, J. Bisquert, I. Ugarte, and R. Pacios, Org. Electron. **9**, 847 (2008).
[16]W. Huang, J. Peng, L. Wang, J. Wang, and Y. Cao, Appl. Phys. Lett. **92**, 013308 (2008).
[17]I. Mora-Sero, J. Bisquert, F. Fabregat-Santiago, G. Garcia-Belmonte, G. Zoppi, K. Durose, Y. Proskuryakov, I. Oja, A. Belaidi, and T. Dittrich, Nano Lett. **6**, 640 (2006).